Enhanced fragmentation of toluene through linear and nonlinear increase of the focal spot area of an ultrashort laser pulse

X. P. Tang,[1] A. Becker,[2] W. Liu,[1,2] M. Sharifi,[1] O. Kosareva,[3] V. P. Kandidov,[3] P. Agostini,[1,4,5] and S. L. Chin[1]
[1]*Centre d'Optique, Photonique et Laser (COPL) and Département de Physique de Génie Physique et d'Optique, Université Laval, Québec, Québec, Canada G1K 7P4*
[2]*Max-Planck-Institut für Physik Komplexer Systeme, Nöthnitzer Strasse 38, D-01187 Dresden, Germany*
[3]*International Laser Center, Department of Physics, Moscow State University, Moscow 119899, Russia*
[4]*Comissariat à l'Energie Atomique, DSM, Centre d'Etudes de Saclay, 91191 Gif-sur-Yvette, France*
[5]*Max-Born-Institut, Max-Born-Strasse 2a, D-12489 Berlin, Germany*
(Received 9 August 2004; revised manuscript received 22 December 2004; published 1 April 2005)

Toluene fragmentation by intense femtosecond laser pulses is experimentally investigated. A strong increase of the toluene fragmentation appears to correlate with an increase of the focal area due to changes in the focal geometry and nonlinear small-scale self-focusing. The scenario of Raman modes excitation proposed in an earlier publication [A.M. Müller *et al.*, Phys. Rev. Lett. **88**, 023001 (2002)] is ruled out as the dominant effect for the enhancement.

DOI: 10.1103/PhysRevA.71.045401 PACS number(s): 33.80.−b, 33.80.Rv, 42.65.−k

The mechanisms leading to the fragmentation of large molecules irradiated by an intense ultrashort near-infrared laser pulse are still far from being elucidated. Such pulses have naturally a large bandwidth and they can, in addition, induce large ac-Stark shifts, which can help in absorbing the large amount of the photons required to reach the fragmentation. Moreover, Coulomb explosion can also lead to the breaking of bonds and the appearance of molecular fragments. There is currently no theoretical approach able to describe to some degree of accuracy fragmentation of large polyatomic molecules due to their interaction with intense laser pulses.

This situation leaves a lot of room for empirical investigations. Recently, for example, the shaping of the pulse field to optimize a given fragment product through a genetic algorithm has been remarkably successful.[1,2] In the case of methyl-benzene, or toluene (C_7H_8), under 800 nm, 80 fs, 10^{14} W/cm^2 pulses, it was suggested[3] that the excitation of active Raman modes of the neutral molecule and/or of the parent ion can result in a considerable enhancement of fragmentation. The excitation of such modes requires that the incident radiation cover a bandwidth wide enough to contain the Raman-shifted frequencies. It is well known that self-phase modulation (SPM) and therefore additional bandwidth can be induced by the Kerr nonlinearity. Müller *et al.*[3,4] (hereafter referred to as I) observed that a long focal lens produced more fragmentation than a short focal lens for a given intensity at the focus and interpreted this fact by the larger amount of SPM induced in the entrance window of the interaction chamber. The data supporting this conclusion are mass spectra taken at various intensities with the long focal length correlated to the laser spectra after the window showing clearly an increase of the bandwidth and a progressive overlap with the active Raman mode frequencies.

The goal of this Brief Report is to show that the enhanced fragmentation rate in the present experiment can be explained by linear and nonlinear changes of the intensity distribution in the focal spot area, while the increase of the pulse bandwidth is not the dominant effect. In order to reach a conclusion, all the changes in the pulse properties have to be controlled. In fact, the same Kerr nonlinearity which produces the changes in the radiation bandwidth also modifies the actual intensity and the size of the interaction through self-focusing of the whole beam as well as small-scale self-focusing. There are clearly multiple possible causes of the same effect and they have to be properly experimentally disentangled.

As in I, our experiment employs a Ti:sapphire laser. It delivers 1.8 mJ, 39 fs (full width at half maximum) pulses with a central wavelength of 800 nm at a repetition rate of 1 kHz. In order to analyze the effects of the self-transformation of the pulses, we compare results obtained using one long focal ($f=500$ mm, CaF_2, 5 mm thick) and one short focal ($f=200$ mm, BK7 glass, 5 mm thick) focusing lens [Figs. 1(a)–1(c)]. Further, the distance between the long focal lens and the entrance window is varied by using an additional pipe of about 300 mm length [Fig. 1(b)]. The 6–mm-thick fused silica input window of the interaction chamber (background pressure 4×10^{-8} Torr) is 15 cm (without pipe) and 45 cm (with pipe) away from the interaction zone. The toluene gas was leaked in at a pressure of 2×10^{-7} to 5×10^{-4} Torr. The parent and fragment ions are detected in a time-of-flight spectrometer.

A measure of the nonlinear self-action effects in the fused silica window is given by the phase change $\varphi_{nl}=(1/2n_0)kn_2|E|^2\Delta z$ across the beam, where k is the wave number, n_2 the nonlinear index ($n_2=3.7\times10^{-16}$ cm^2/W for fused silica[6]), E the electric field of the wave, and Δz the propagation distance. We estimate φ_{nl} to be about 1.6π for a 700 μJ pulse [corresponding to a peak intensity of $I=(c/8\pi)|E|^2=10^{12}$ W/cm^2 on the window] when using the long focal lens without pipe. In comparison, the nonlinear phase change in the focusing lens and in the air path in between the optical elements is more than an order of magnitude smaller and, hence, negligible. In both of the other experimental setups, the total phase change is much smaller and, hence, self-action effects are negligible.

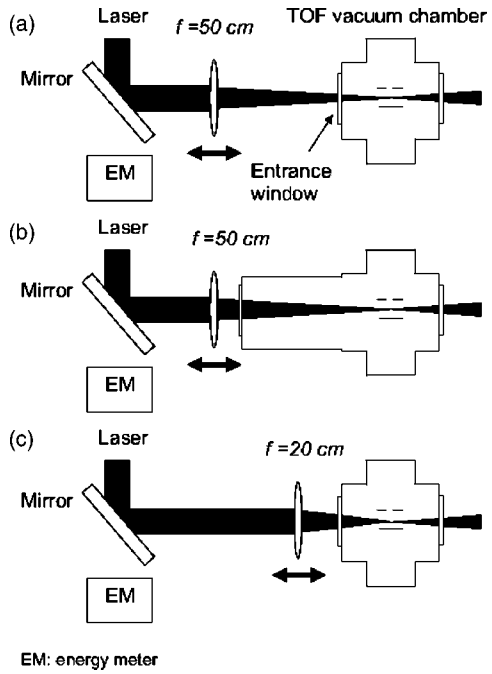

FIG. 1. Experimental setups. The length of the focusing lens and the position of the entrance window with respect to the lens are changed in order to vary the strength of the self-action effects in the window. (a) $f=500$ mm, large distance between lens and window (strong self-action effects), (b) $f=500$ mm, small distance between lens and window (small self-action effects), and (c) $f=200$ mm, short distance between lens and window (small self-action effects).

The changes in the pulse spectrum and in the beam geometry as well as the methods used to record them are described in detail in Ref. 5. When crossing the input window, the beam undergoes first, indeed, a self-transformation due to self-phase modulation in the case of the longer focal length. The spectral broadening is, however, quite small in our case [Figs. 2(a) and 2(b)]: at the 50% level, there is practically no change of the spectral width. However, we do observe a very substantial enhancement of the fragmentation rate for the longer focal lens, as can be seen from the corresponding mass spectra in Fig. 3. Please note that all spectra are normalized to the same intensity of the parent ion and the spectra in the same row are recorded at (almost) the same averaged laser intensity.

Most interestingly, for the longer focal lens, the amount of fragmentation does not change significantly with or without the pipe. This indicates that the main origin for the enhanced fragmentation rate for the longer lens results from the change of the focusing geometry. This is further substantiated by the results of model calculations for the ratio of the yield of one fragment (CH^+) to the yield of the parent ion. The parent ion and fragment yields are determined by solving the set of rate equations,

$$\frac{dP_0(\vec{r},t)}{dt} = -\Gamma^+(I(\vec{r},t))P_0(\vec{r},t),$$

$$\frac{dP_{\text{ion}}(\vec{r},t)}{dt} = \Gamma^+(I(\vec{r},t))P_0(\vec{r},t) - \Gamma_{CH^+}(I(\vec{r},t))P_{\text{ion}}(\vec{r},t),$$

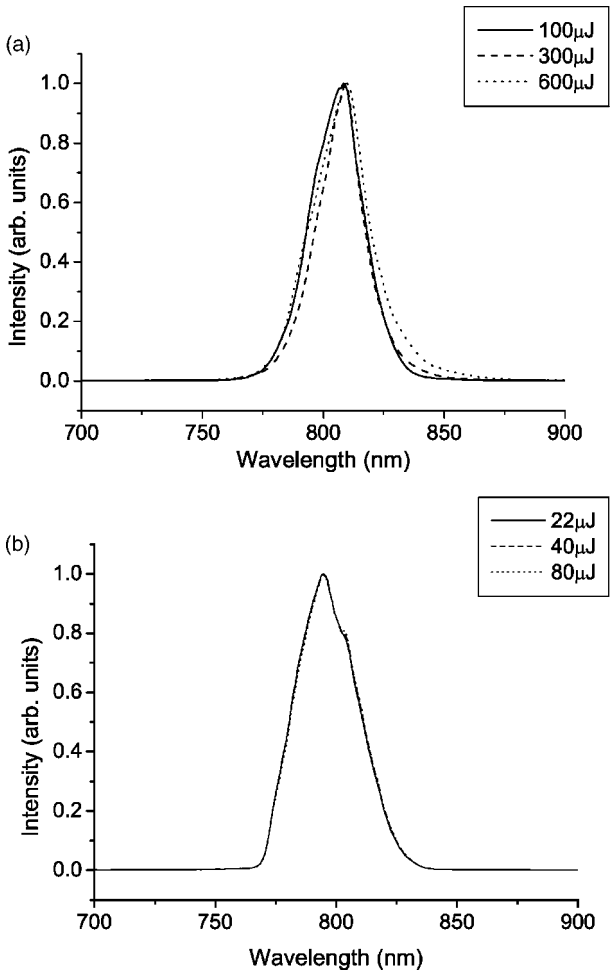

FIG. 2. Pulse spectra at different input energies, obtained using the $f=500$ mm lens, (a) without pipe. (b) Same, but for the $f=200$ mm lens. Note that in panel (b), the different curves coincide.

$$\frac{dP_{CH^+}(\vec{r},t)}{dt} = \Gamma_{CH^+}(I(\vec{r},t))P_{\text{ion}}(\vec{r},t).$$

The equations are solved using the initial condition $P_0=1$ and $P_{\text{ion}}=P_{CH^+}=0$, and integrated over the contributions in the focus. The rate of single ionization, Γ^+, is calculated using the first-order intense-field *S*-matrix theory.[7] The rate of fragmentation, Γ_{CH^+}, is determined empirically, such that the numerical result for the ratio P_{CH^+}/P_{ion} equals the experimental value for the $f=200$ mm lens, assuming an undisturbed Gaussian intensity distribution and a detector opening of 1.2 cm. Using this empirical fragmentation rate, we have performed calculations for the $f=500$ mm lens using an undisturbed Gaussian distribution (experimental setup with pipe) and the simulated nonlinear intensity distribution [Fig. 1(a), experimental setup without pipe]. Modelization of the intensity distribution has been done using a pulse propagation model. The numerical results corresponding to the input energies in the lower row of Fig. 3 are in agreement with the experimental data (Table I). Thus, the enhancement of the fragment yields (relative to the parent ion yield) in our experimental setup is due to the larger focal spot area in the

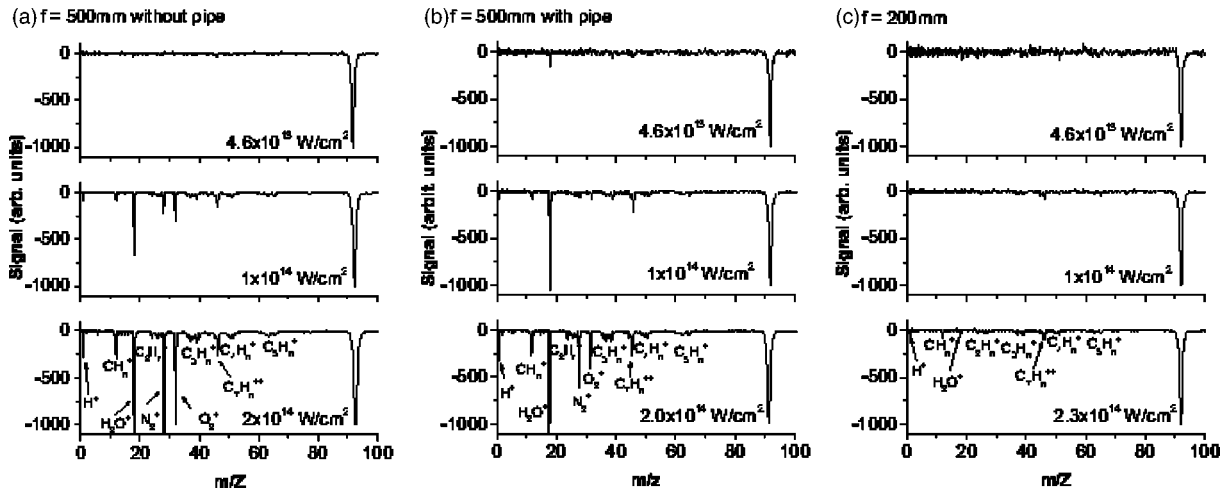

FIG. 3. Mass spectra of toluene molecule obtained (a) with $f=500$ mm lens without pipe, (b) with $f=500$ mm lens with pipe, and (c) with $f=200$ mm lens. Spectra in the same row are recorded at (almost) the same averaged intensity. Note the energy-intensity calibration: (a) 4.6×10^{13} W/cm^2 (112 μJ), 10^{14} W/cm^2 (268 μJ), 2×10^{14} W/cm^2 (529 μJ); (b) 4.6×10^{13} W/cm^2 (120 μJ), 10^{14} W/cm^2 (200 μJ), 2×10^{14} W/cm^2 (426 μJ); (c) 4.6×10^{13} W/cm^2 (17 μJ), 10^{14} W/cm^2 (35 μJ), 2×10^{14} W/cm^2 (74 μJ).

case of the longer focal length. As a result, above saturation the low-intensity parts, where the parent ions are created, move quickly outside the effective interaction zone (seen by the detector), while the fragments are created at the center of the interaction zone. As a result, the observed fragmentation rate seems to increase. This effect is further enhanced when there is an additional nonlinear increase of the focal spot area due to small-scale self-focusing effects, as for the 500 mm lens without pipe. Figure 4(a) shows the simulated focal spot region for the input pulse energy of 50 μJ. There is no self-focusing for this comparatively low energy. At a higher energy of 600 μJ, self-focusing in the chamber window leads to the distortion and broadening of the focal spot area [Fig. 4(b)].

We finally examine the possible role of the Raman mode excitation invoked in I. On the one hand, because of its shorter duration, our pulse spectrum is wide enough to encompass the Raman transitions at all energies. On the other hand, the increase of the spectral density at the Raman frequencies is marginal for pulses with energies in the range 200–500 μJ, where the fragmentation rate increases enormously. Note that the simple increase of the spectral density at the Raman frequencies due to the increase of the pulse energy is ruled out since the increase in the fragmentation rate observed with the short focal length is much smaller than for the long focal length, while the spectral content is obviously the same.

TABLE I. Comparison of experimental data and results of numerical simulation for the ratio P_{CH^+}/P. The input energies are as in Fig. 3, lower row.

Focal distance	Experiment	Simulations
$f=200$ mm	0.06	0.06
$f=500$ mm, with pipe (Gaussian distribution)	0.26	0.19
$f=500$ mm, without pipe (distorted distribution)	0.30	0.32

In summary, we observe a drastic enhancement of the fragmentation of toluene correlated to linear (focusing geometry) and nonlinear (small-scale self-focusing) increase of the focal spot area. The excitation of the Raman modes proposed in an earlier publication does not appear to be the dominant reason.

This work has been supported in Canada by the Canadian Research Chairs, the Canadian Foundation for Innovation (CFI), NSERC, DRDC-Valcartier, CIPI, Spectra Physics, and FQRNT. V.P.K. and O.G.K. acknowledge the support of the Russian Foundation for Basic Research, Grant No. 03-02-16939; V.P.K., O.G.K., and S.L.C. acknowledge the support of the NATO Linkage Grant No. PST.CLG.976981. P.A. gratefully acknowledges support from the COPL during the Fall-Winter 2002–2003. Support of the Alexander von Humboldt Foundation to P.A. and S.L.C. is highly appreciated.

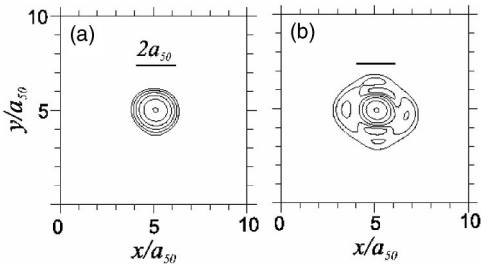

FIG. 4. Results of numerical calculations for the fluence distribution in the focal area using an $f=500$ mm lens (without pipe) at (a) 50 μJ and (b) 600 μJ. The lowest contour value is 0.03 of the maximum contour value in all panels. The interval between the contours changes as 2^n, where n is the contour number. Horizontal scale indicates the diameter $2a_{50}$ of the fluence distribution obtained at 50 μJ at the $1/e^2$ level.

[1] A. Assion, T. Baumert, M. Bergt, T. Brixner, B. Kiefer, V. Seyfried, M. Strehle, and G. Gerber, Science **282**, 919 (1998).
[2] R. J. Levis, G. M. Menkir, and H. Rabitz, Science **292**, 709 (2001).
[3] A. M. Müller, B. Witzel, C. J. G. J. Uiterwaal, J. Wanner, and K. L. Kompa, Phys. Rev. Lett. **88**, 023001 (2002).
[4] A. M. Müller, C. J. G. J. Uiterwaal, B. Witzel, J. Wanner, and K. L. Kompa, J. Chem. Phys. **112**, 9289 (2000).
[5] X. P. Tang, A. Becker, W. Liu, M. Sharifi, O. Kosareva, V. P. Kandidov, P. Agostini, and S. L. Chin, Appl. Phys. B(to be published).
[6] R.L. Sutherland, *Handbook of Nonlinear Optics* (Marcel Dekker, New York, 2003).
[7] J. Muth-Böhm, A. Becker, S. L. Chin, and F. H. M. Faisal, Chem. Phys. Lett. **337**, 313 (2001).